

RAPIDLY DEPOSITED HOT-WIRE CVD SILICON NITRIDE AS PASSIVATING ANTIREFLECTION COATING ON SOLAR CELLS

V. Verlaan¹, C.H.M. van der Werf¹, Z.S. Houweling¹, Y. Mai¹, R. Bakker¹,

I.G. Romijn², A.W. Weeber², H.D. Goldbach¹, and R.E.I. Schropp¹

Abstract— Hot-wire chemical vapor deposition (HWCVD) is a promising technique for very fast deposition of high quality thin films. We investigated silicon nitride (SiN_x) deposited with HWCVD as passivating antireflection coating (ARC) at a high deposition rate of 180 nm/min. Series of multi-crystalline silicon (mc-Si) solar cells were made using HWCVD SiN_x with different atomic compositions. The open circuit voltage (V_{oc}) and the short circuit current density (J_{sc}) have an optimum at an N/Si ratio (x) of 1.31. At this composition, the best solar cells reached an efficiency of 15.7 %, close to the best reference cell with optimized microwave PECVD SiN_x (16.1%). The optimum at N/Si = 1.31 is explained by the high mass density, which peaks at this composition. Internal Quantum Efficiency (IQE) measurements at 1000 nm confirm this optimum and prove good bulk passivation. The IQE at a wavelength of 400 nm shows a combined optimal effect of surface passivation and absorption. The optimal N/Si ratio of 1.31 is significantly higher than the values reported for PECVD coatings (1.0). This higher N/Si ratio for HWCVD films leads to a larger bandgap and thus lower light absorption. Consequently, a higher IQE blue response and a slightly higher J_{sc} are obtained with HWCVD SiN_x coatings.

Index Terms— Silicon nitride, Hot-wire CVD, Multi-crystalline Solar Cells, Antireflection coating

I. INTRODUCTION

A thin (~80 nm) SiN_x film on top of a multi-crystalline silicon (mc-Si) solar cell has a large influence on the performance of such a cell. Firstly, the SiN_x acts as an effective antireflection coating (ARC) because of its intermediate and tunable refractive index in combination with a low extinction coefficient.

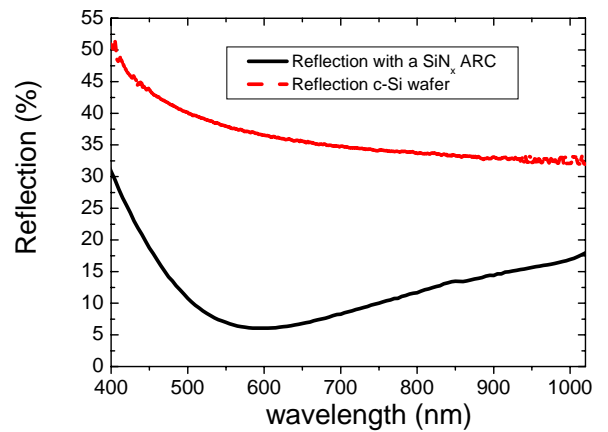


Figure 1: Reflection of a c-Si wafer with and without an SiN_x ARC.

The reflection (R_{ij}) at the interface between two layers i and j depends on their refractive indices (n_i and n_j) for light with wavelength (λ) by:

$$R_{ij}(\lambda) = \left(\frac{n_i(\lambda) - n_j(\lambda)}{n_i(\lambda) + n_j(\lambda)} \right)^2 \quad (1)$$

From equation 1 it can be concluded that at an interface with two materials with a large difference in refractive indices, the reflection will be high. Since the refractive index difference between air (1.0) and the Si-wafers (3.42) is relatively large, a large portion of the incoming light is reflected. By adding a SiN_x layer, with a refractive index between that of air and Si, the reflection is greatly reduced. Furthermore, by optimizing the interference of the incoming light according to

$$\frac{1}{4} \lambda = n(\lambda)d \quad (2)$$

with d the thickness of the SiN_x layers, the minimum in reflection can be tuned to the wavelengths where the maximum in the solar intensity is present. Typical reflection (at the

¹Utrecht University, Faculty of Science, Department of Physics and Astronomy, SID - Physics of Devices, P.O. Box 80 000, 3508 TA Utrecht, the Netherlands. email: V.Verlaan@phys.uu.nl

²ECN Solar Energy, P.O. Box 1, NL 1755 ZG Petten, the Netherlands. The authors thank SenterNovem for partial financial support

various wavelengths) with and without a SiN_x ARC can be observed in Figure 1.

Dangling Si bonds, crystal-defects and impurities in the bulk of silicon create energy levels within the bandgap and act as recombination centers for the light induced charge carriers. Furthermore, there are also dangling bonds at the Si/ SiN_x interface. Fortunately, these defects and impurities can be passivated with atomic hydrogen coming from the SiN_x coating. Passivation occurs after a brief high-temperature anneal, during which the atomic hydrogen is released from the SiN_x film and diffuses into the wafer.

For commercial cell production, plasma enhanced chemical vapor deposition (PECVD) is most frequently used for deposition of SiN_x . However, in recent years, a totally plasma-free deposition technique, hot-wire (HW) CVD, has been attracting much interest [1-5]. Using the HWCVD technique, the source gasses are catalytically decomposed at resistively heated filaments into radicals only. This decomposition takes place with very high efficiency [6]. Since neither ions nor strong electric fields are present, HWCVD prevents the substrate from damage caused by ion bombardment [7] as is the case with direct PECVD systems.

For commercial application, the deposition rate is becoming increasingly important. From a cost perspective, an effective way to reduce the production costs of module manufacturing is by increasing the throughput. The most straightforward way to achieve this is by an increase of the deposition rate. It has been shown that high quality SiN_x can be obtained at ultra high deposition rates of over 7 nm/s using HWCVD [8,9]. This deposition rate is much faster than current commercial deposition techniques are offering [10-12]. Additional benefits of HWCVD deposited SiN_x films for solar cell production are the very low stress of 50 MPa [13] and the very high gas utilization rate (>75%) [14]. The low stress prevents blistering of the coatings during the high-temperature steps in solar cell production, such as firing of the metal contacts.

In this paper we report on HWCVD SiN_x on mc-Si solar cells as passivating ARC. We show that the optimal composition for HWCVD SiN_x occurs at N/Si = 1.31. Furthermore, we will show that despite a much higher deposition rate, SiN_x deposited by hot-wire CVD enables solar cell results that are comparable to those obtained with optimized microwave (MW) PECVD.

II. EXPERIMENTAL DETAILS

All depositions were performed in a four-filament hot-wire reactor that is part of an ultra high vacuum multi chamber system. As source gasses pure silane (SiH_4) and ammonia (NH_3) were used, which are decomposed at resistively heated tantalum filaments held at 2100 °C. No additional substrate heating was applied. In this laboratory system, a shutter is situated between the sample and the wires to control the duration of the deposition. This experimental reactor contains a uniform deposition area of $5 \times 5 \text{ cm}^2$. Scaling up of the

HWCVD technique towards larger areas is considered to be straightforward [15,16] since there is no fundamental limit to the size of the vacuum chamber and the extent and multitude of heated wires.

Depositions were performed simultaneously on Corning glass 1737F and crystalline Si wafers. The layers were characterized by reflection/transmission measurements [17,18] to determine the optical properties (refractive index, absorption), elastic recoil detection (ERD) [19] and Rutherford backscattering (RBS) [20] were used to obtain compositional properties and absolute atomic densities.

The HWCVD SiN_x coatings were tested in the standard industrial cell processes of ECN Solar Energy [21,22]. For cell optimization, various series of HWCVD SiN_x with different compositions were deposited on mc-Si wafers as supplied by ECN Solar Energy. After completion of the HWCVD SiN_x depositions, the wafers were transported back to ECN for metallization at the front and backside. For comparison and reference, solar cells made from neighboring wafers using optimized remote MW PECVD SiN_x were provided. To evaluate the surface passivation, lifetime measurements were performed using a quasi-steady-state photoconductance measurement setup [23] on $5.8 \text{ } \Omega\text{cm}$ mono-crystalline Si wafers with HWCVD SiN_x deposited on both sides. The rough crystalline wafers were chemically etched and received an HF dip prior to the HWCVD SiN_x deposition. The HWCVD SiN_x coatings (~300 nm) with equal composition were deposited on both sides of the wafer.

III. RESULTS AND DISCUSSION

3.1 Layer analysis

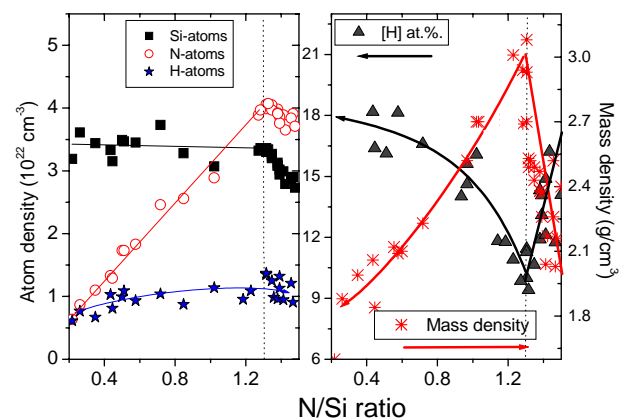


Figure 2: (a) The atomic densities in SiN_x with various compositions. (b) The mass density and hydrogen concentrations. Both show a strong dependence on the composition. The line are a guide to the eye.

Figure 2 (a) shows the volume densities of the present atoms as a function of N/Si. It is of interest that the density of Si and H atoms for films below N/Si = 1.31 is invariable. For this regime, the difference in composition is only caused by

differences in the volume density of N. For films with $N/Si > 1.31$, both the N and Si atom densities decrease, whereby the Si density decreases faster than the N density. This decrease in atom densities is caused by the formation of voids in the films. These voids are observed by TEM pictures [24].

The absolute H density shows a very small increase with increasing N/Si over the whole range of compositions. Thus, both the composition and the relative atomic hydrogen concentration of the deposited films depend primarily on the amount of incorporated N atoms in the films.

Using the atomic densities as derived using ERD and RBS measurements, the mass density of the films can be obtained. Since the main difference in the films is the N density also the mass density depends mainly on the composition of the films. The correlation between the mass density and composition is shown in Figure 2(b). As expected, the mass density increases with increasing N/Si reaching a maximum at the point where also the nitrogen density peaks. For films with $N/Si > 1.31$ the mass density decreases caused by a decrease in N and Si density. The same trend is (indirectly) reported for conventional PECVD SiN_x , though with the difference that for PECVD the maximum in mass density is reached at $N/Si = 1.0$ [25]. Thus using HWCVD SiN_x , films with high mass density can be obtained that are close to stoichiometry. The mass density reached 3.0 g/cm^3 for films with $N/Si = 1.31$, which is comparable to the most compact, though Si-rich films reported for PECVD depositions [26].

3.2 Solar cell results

In Figure 3(a), the average V_{oc} values relative to the reference group are plotted for each series of cells containing different compositions of SiN_x . Each series contains the average over 5 cells. A clear trend can be observed in which a maximum of V_{oc} is reached for a N/Si value of 1.31. Also the average J_{sc} is shown for each series. Again a clear trend is visible as a function of the N/Si ratio, the optimal result again at a N/Si ratio of 1.31.

The best solar cell reached an efficiency of 15.7 % with a V_{oc} of 604 mV and J_{sc} of 34.6 mA/cm^2 . These values are very close to the best values obtained in the reference group. To our knowledge, the 15.7 % reported in this paper is the best efficiency for HWCVD SiN_x on mc-Si solar cells [7].

The 15.7% conversion efficiency is comparable to that for optimized PECVD SiN_x , though the HWCVD SiN_x is made at a much higher deposition rate (3 nm/s for HWCVD, versus 1 nm/s for MW PECVD).

	V_{oc} (mV)	J_{sc} (mA/cm^2)	FF	eff (%)
HWCVD CVD best	604	34.6	0.750	15.7
MW PECVD best	606	34.3	0.774	16.1

Table 1: Best solar cell results for cells with HWCVD SiN_x and the reference cells.

The main difference with the reference cells is found in the FF. In all cells the FF of the HWCVD deposited SiN_x cells is lower than the reference cells. This difference is caused by unoptimized cell processing for the cells with HWCVD SiN_x , such as firing conditions. For example HWCVD deposited SiN_x has a higher mass density [27,28] and may therefore necessitate different firing parameter settings for optimal FF.

The internal quantum efficiency (IQE) measurements provide a more detailed insight in the passivation properties of HWCVD SiN_x . Figure 3(b) shows the IQE at 400 and 1000 nm. The IQE values are only slightly lower in the infrared region, however still proving good bulk passivation. By comparing the relative IQE results for each N/Si , a confirmation is found that the optimal HWCVD SiN_x has a N/Si ratio of 1.31.

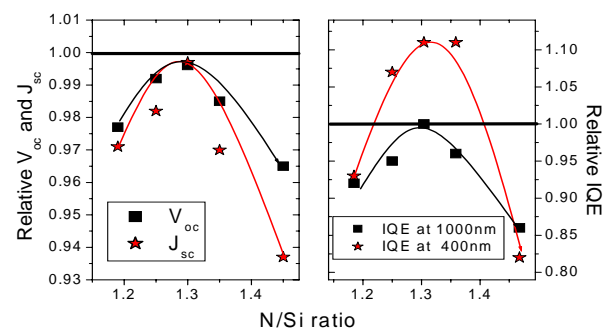


Figure 3: The relative V_{oc} and J_{sc} values for mc-Si solar cells containing different HWCVD SiN_x compositions. The highest values are obtained at $N/Si = 1.31$. Interesting is the higher blue response for the HWCVD SiN_x coatings. The lines are a guide to the eye.

It is remarkable that the IQE values for wavelengths smaller than 600 nm for the cells with HWCVD SiN_x were significantly better than for those with optimized PECVD SiN_x . This occurred in a wide range of compositions. The better blue response could originate from two effects, i.e. better surface passivation or lower blue absorption in the HWCVD SiN_x layers. To find the origin of this difference, the optical absorption of the layers was compared. The comparison revealed that the absorption of the two types of layers is indeed different. The absorption of the HWCVD nitrides showed to be negligible, caused by the relatively high N/Si ratio, whereas MW PECVD SiN_x showed an extinction coefficient at 400 nm (k_{400nm}) of 0.03.

To quantify the effect of the absorption, simulations with PC-1D (version 5.5) [30] were performed at ECN, taking into account this difference in absorption. From the results it appeared that the surface recombination velocity for the cells with HWCVD SiN_x and with MW PECVD was identical. We therefore conclude that the better blue response is caused by the much lower absorption in the HWCVD SiN_x layers. The PC-1D simulations also reveal that the cells with HWCVD SiN_x have a high minority carrier lifetime, only slightly lower than that of the reference cells deposited with MW PECVD. This confirms that good bulk passivation is obtained using HWCVD.

Figure 4(a) shows the lifetimes of the wafers as deposited. The lifetimes presented in this paper are taken at an injection level of 10^{15} cm^{-3} . It clearly shows that without a “firing” anneal step the most Si-rich films lead to the best surface passivation.

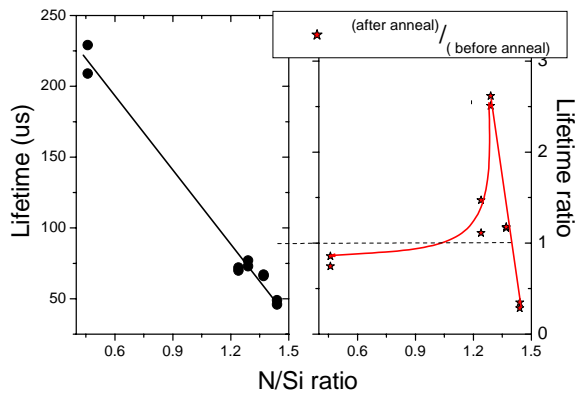


Figure 4: (a) Lifetimes for different compositions of HWCVD SiN_x . (b) The ratio of lifetimes before and after firing.

The measurements were repeated on the same wafers after a firing treatment. This firing step was performed to initiate hydrogen passivation originating from the SiN_x layer. Figure 4(b) shows that the structures with a N/Si of around 1.31 have the largest improvement by a factor of 2.5. The lifetime obtained corresponds to a surface recombination velocity of 54 cm/s , which is comparable to values reported for solar cell grade SiN_x coatings deposited using remote PECVD systems [10,31]. The optimum in hydrogen passivation is a second confirmation of the optimum of the HWCVD SiN_x coatings at N/Si = 1.31.

The optimal N/Si ratio of 1.31 for hydrogen passivation is significantly higher than values reported for plasma SiN_x ARCs where optimum N/Si ratios of roughly 1.0 are reported [32]. This difference is probably caused by a different optimum in mass density of the HWCVD SiN_x films compared to the PECVD SiN_x coatings.

Several studies have shown that mass density has a large influence on the bulk passivating properties of the SiN_x [26,28,33,34]. Also this study (Fig. 5) shows a clear correlation between the mass density and the passivating properties. Although no conclusive model for hydrogen passivation has been presented yet, it is generally accepted that a low mass density facilitates hydrogen removal through the formation of H_2 [35,36]. This molecular hydrogen cannot contribute to hydrogen passivation, thus films with a more open structure show a reduced passivation effect. SiN_x layers with a higher mass density contain fewer and/or smaller voids preventing cross-linking reactions and thereby promoting diffusion of atomic hydrogen. It has been proposed though, that too dense layers may cause slower atomic hydrogen diffusion and thus reduction in passivation [36].

In this study there is no indication for an optimum in mass density since the best results are obtained for samples with the highest obtained mass density. A detailed study of the hydrogen

movement in these dense layers shows that this hydrogen transport occurs mainly by N-H bonded hydrogen [37].

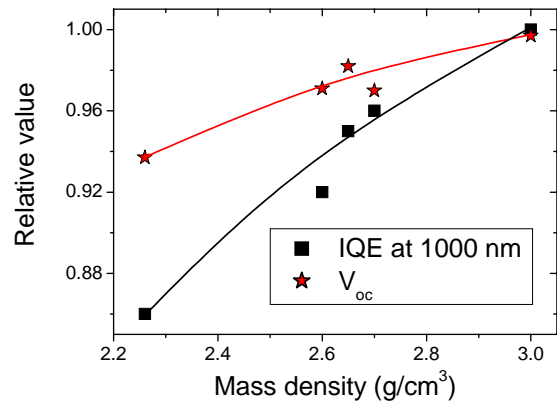


Figure 5: The normalized V_{oc} and IQE for different densities. The best passivation was obtained for the most dense layers.

IV. CONCLUSION

We developed silicon nitride deposited with HWCVD as passivating antireflection coating at a high deposition rate of 3 nm/s . Series of multi-crystalline silicon solar cells were made using different compositions of HWCVD SiN_x . Both the V_{oc} and the J_{sc} have a clear optimum at an atomic N/Si ratio at 1.31. The IQE measurements show that an optimum is achieved at N/Si = 1.31. This optimum is probably caused by the mass density, which peaks at this composition. At this composition, the best solar cells reached an efficiency of 15.7 %, which is close to the best PECVD reference cell (16.1%).

The optimal N/Si ratio of 1.31 value is significantly higher than the values reported for PECVD coatings (1.0). This higher N/Si ratio leads to a larger band gap and thus lower light absorption. Since the HWCVD sample have a much significant higher N/Si than the reference films, most likely the difference in absorption is caused by differences in bandgaps. Consequently, a higher blue response and a slightly higher J_{sc} are obtained for HWCVD SiN_x coatings. PC-1D simulations and lifetime measurements confirm the good bulk and surface passivation, respectively.

In conclusion, HWCVD SiN_x as passivating antireflection layer on mc-Si solar cells leads to efficiencies comparable to those with optimized PECVD SiN_x coatings, though HWCVD is performed at a much higher deposition rate.

ACKNOWLEDGMENT

We thank SenterNovem for partial financial support, and Wim Arnold Bik (Utrecht University) for help with the ion beam analysis. We thank Simona de Iuliis (ECN Solar Energy) for the lifetime measurements.

REFERENCES

- [1] B. Stannowski, J.K. Rath, and R.E.I. Schropp. Thin Solid Films 395 (2001) 339.

- [2] A.H. Mahan, A.C. Dillon, L.M. Gedvilas, D.L. Williamson, and J.D. Perkins. *J. Appl. Phys.* 94 (2003) 2360
- [3] J.K. Holt, D.G. Goodwin, A.M. Gabor, F. Jiang, M. Stavola, and H. Atwater. *Thin Solid Films* 430 (2003) 37.
- [4] F. Liu, S. Ward, L. Gedvilas, B. Keyes, Q. Wang, E. Sanchez, and S. Wang. *J. Appl. Phys.* 96 (2004) 2973.
- [5] M. Kitazoe, S. Osono, H. Itoh, S. Asari, K. Saito, and M. Hayama. *Thin Solid Films*. 501 (2006) 160.
- [6] S.G. Ansari, H. Umamoto, T. Morimoto, K. Yoneyama, A. Izumi, A. Masuda, H. Matsumura. *Thin Solid Films* 501 (2006) 31
- [7] V. Verlaan, C.H.M. van der Werf, Z.S. Houweling, I.G. Romijn, A.W. Weeber, and H.D. Goldbach, and R.E.I. Schropp. *Progr. Photovolt: Res. Appl.* 15 (2007) 563-573.
- [8] V. Verlaan, Z.S. Houweling, C.H.M. van der Werf, H.D. Goldbach, R.E.I. Schropp. *MRS Proceedings* 910 (2006) 61
- [9] J.D. Moschner, J. Schmidt and R. Hezel. *Proc. 19th Photovoltaic Solar Energy Conference*. Paris, 2004. 1082,
- [10] B. Hoex, A.J.M. van Erven, R.V.M. Bosch, W.T.M. Stals, M.D. Bijker, P.J. van den Oever, W.M.M. Kessels and M.C.M. van de Sanden. *Progr. Photovolt: Res. Appl.* 13 (2005) 705
- [11] S. von Aichberger. *PHOTON international* 3 (2004) 40
- [12] K. Schade, F. Stahr, J. Kuske, S. Rohlecke, O. Steincke, U. Stephan, H.F.W. Dekkers. *Thin Solid Films* 502 (2006) 59
- [13] Z.S. Houweling, V. Verlaan, C.H.M. van der Werf, H.D. Goldbach, R.E.I. Schropp. *MRS Proceedings* 989 (2007) A4.5 .
- [14] R.E.I. Schropp, S. Nishizaki, Z.S. Houweling, V. Verlaan, C.H.M. van der Werf, and H. Matsumura. Accepted for publication in *Solid State Electronics*.
- [15] A. Lederman, U. Weber, C. Mukherjee, B. Schroeder. *Thin Solid Films* 395 (2001) 61.
- [16] H. Matsumura and K. Ohdaira. *Extended Abstract Book. 4th International Conference on Hot-Wire CVD Process*. Gifu, Japan. October 2006, page 195
- [17] S.G. Tomlin, *J. Phys. D* 5 (1972) 847.
- [18] Y. Hishikawa, N. Nakamura and Y. Kuwano. *Jpn. J. Appl. Phys.* 30 (1991) 1008
- [19] W.M. Arnold Bik and F.H.P.M. Habraken. *Rep. Prog. Phys.* 56 (1993) 859
- [20] W.K. Chu, J.W. Mayer, and M.A. Nicolet. *Backscattering Spectrometry*. (Academic, New York, N.Y, USA, 1978)
- [21] A.W. Weeber, A.R. Burgers, M.J.A.A. Goris, M. Koppers, E.J. Kossen, H.C. Rieffe, W.J. Soppe, C.J.J. Tool and J.H. Bultman. *Proc. 19th Photovoltaic Solar Energy Conference*, Paris. 532.
- [22] A.W. Weeber, R. Kinderman, P.C. de Jong, and C.J.J. Tool. *Proc. 21th Photovoltaic Solar Energy Conference*, Dresden. 605.
- [23] R.A. Sinton and A. Cuevas, *Appl. Phys. Lett.* 69 (1996) 2510.
- [24] B. Stannowski, J.K. Rath, and R.E.I. Schropp. *J. Appl. Phys.* 93 (2003) 2618.
- [25] S. Hasegawa, L. He, Y. Amano, and T. Inokuma. *Physical Review B*. 48 (1993) 5315.
- [26] H.F.W. Dekker, L. Carnel, and G. Beaucarne. *Appl. Phys. Lett.* 89 (2006) 013508.
- [27] W.J. Soppe, J. Hong, W.M.M. Kessels, M.C.M. van der Sanden, W.M. Arnoldbik, H. Schlemm, C. Devilee, H. Riefe, S.E.A. Schiermeier, J.H. Bultman and A.W. Weeber. *IEEE PVSC 2002 New Orleans*. 189, 104.5.
- [28] J. Hong, W.M.M. Kessels, W.J. Soppe, A.W. Weeber, W.M. Arnoldbik, and M.C.M. Sanden, *J. Vac. Sci. Technol B* 21 (2003), 2123.
- [29] C.J.J. Tool, G. Coletti, F.J. Granek, J. Hoornstra, M. Koppes, E.J. Kossen, H.C. Rieffe, I.G. Romijn, and A.W. Weeber. *Proc. 20th Photovoltaic Solar Energy Conference*. Barcelona, 2005.
- [30] P.A. Basore and D.A. Clugston, *PC1D v5.5* (University of New South Wales, Sydney, Australia, 2000).
- [31] J.D. Moschner, J. Henze, J. Schmidt, and R. Hezel, *Progr. Photovolt: Res. Appl.* 12 (2004) 21
- [32] H.F.W. Dekkers, L. Carnel, G. Beaucarne, and W. Beyer. *Proc. 20th Photovoltaic Solar Energy Conference*. Barcelona, 2005.
- [33] A.W. Weeber, H.C. Rieffe, I.G. Romijn, W.C. Sinke, and W.J. Soppe. *Proc. 31st IEEE PVSEC Florida* 2005.
- [34] D. Benoit, J. Regolini, and P. Morin. *Microelectronic Engineering* 84 (2007) 2169.
- [35] H.F.W. Dekkers, G. Beaucarne, H. Miller, H. Charifi, and O. Slaoui. *Appl. Phys. Lett.* 89 (2006) 211914.
- [36] I.G. Romijn, W.J. Soppe, H.C. Rieffe, W.C. Sinke, and A.W. Weeber. *Proc. 20th Photovoltaic Solar Energy Conference*. Barcelona, 2005.
- [37] V. Verlaan, C.H.M. van der Werf, W.M. Arnoldbik, H.D. Goldbach, and R.E.I. Schropp. *Phys. Rev. B* 73 (2006) 195333.